Expansion Measurements of Tycho's Supernova Remnant and Their Implications of the Progenitor System

Takaaki Tanaka[1], Hiroyuki Uchida[2], Tomoaki Kasuga[3], Shiu-Hang Lee[2], Keiichi Maeda[2], Hiroya Yamaguchi[4,3], Brian J. Williams[5], Aya Bamba[3]

[1]Konan University, [2]Kyoto University, [3]University of Tokyo, [4]ISAS/JAXA, [5]GSFC/NASA,

1. Introduction

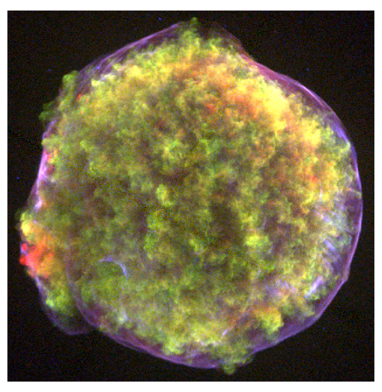

Figure 1. Three color image of Tycho's SNR obtained with Chandra ACIS.

Tycho's supernova (SN) or SN 1592 is known to be a standard type Ia explosion based on the X-ray spectroscopy of its supernova remnant (SNR) (Badenes et al. 2006) and on the observations of light echoes. One of the burning questions about type Ia supernovae is what kind of progenitor systems lead to explosions. Two scenarios are discussed in the literature. One is the single-degenerate (SD) scenario, in which mass accretion from a non-degenerate companion onto a white dwarf leads to an explosion. In the other scenario, called the double-degenerate (DD) scenario, a merger of two white dwarfs forming a binary system triggers an explosion. The environment of supernova remnants, e.g., ambient density structure, is one of the keys to answering this question. In the SD scenario, a strong wind is expected to blow from the progenitor system in the pre-SN phase (e.g., Hachisu et al. 1996), which may leave a cavity-like structure. In the DD scenario, on the other hand, such an outflow generally is not anticipated. We here report on our X-ray imaging ad spectral analyses of Tycho's SNR (Figure 1), aiming to probe its ambient gas environment.

2. Imaging Analysis with Chandra

To measure the expansion rate of Tycho's SNR, we generated 4.1–6.1 keV band flux images for each of the 2003, 2009, 2009, and 2015 data obtained with Chandra. The image taken in 2009 is presented in Figure 1a. The emission in this energy band is dominated by synchrotron emission from accelerated electrons, and is selected here since the rim structures are most clearly visible in this band.

We measured expansion rate of the remnant in 13 regions indicated in Figure 2a. In Figure 2b, we show projection along the shock front in Region 8 obtained in 2003 and 2009, where expansion is clearly visible. We shifted one dataset at some step, and, at each step, we calculated chi-squared values between the two datasets. From the obtained chi-squared as a function of shift, we obtained the shift which gives the minimum chi-squared and thus is the best estimated value.

The top panel of Figure 2c shows the expansion velocities measured in each of the 13 regions in three different time intervals. In the bottom panel, we plot acceleration under an assumption that it is constant between 2003 and 2015. In earlier times, expansion is faster in the southern and western regions (see the velocities measured in 2003–2007). The expansion in these regions decelerated over the years. The measurement in the 2009–2015 interval indicates that the expansion of the 13 regions reach almost a common velocity. The result suggest that the blast wave recently hit a dense gas wall.

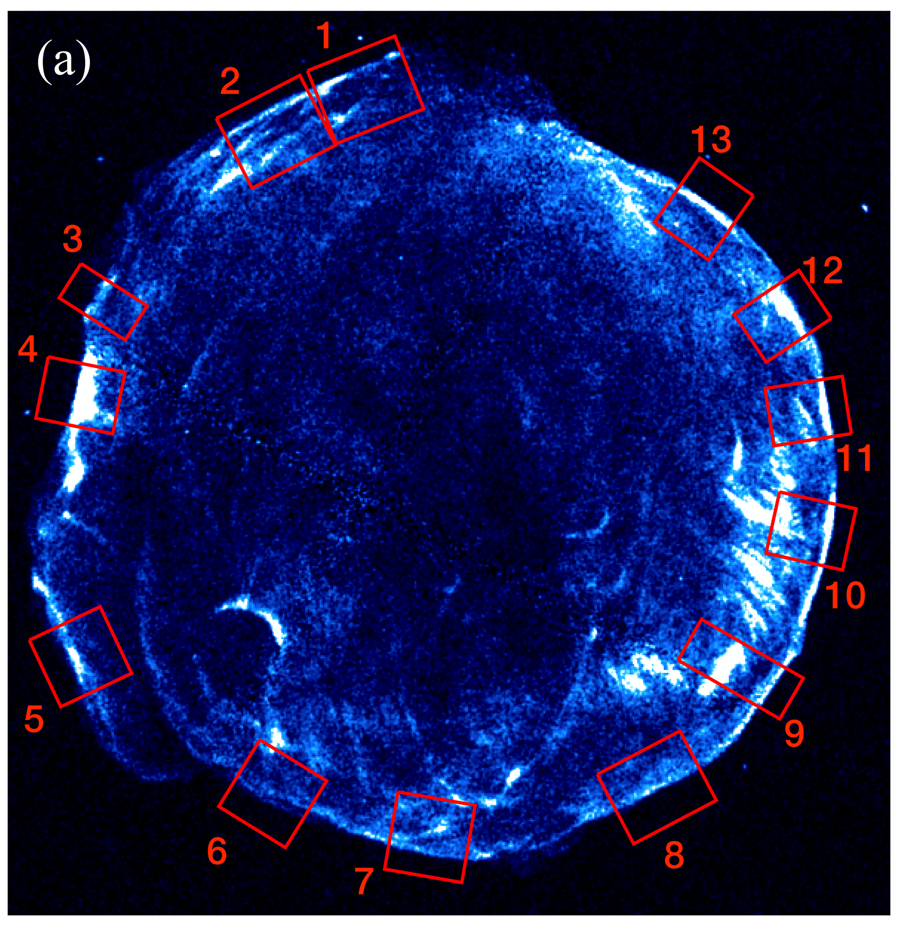

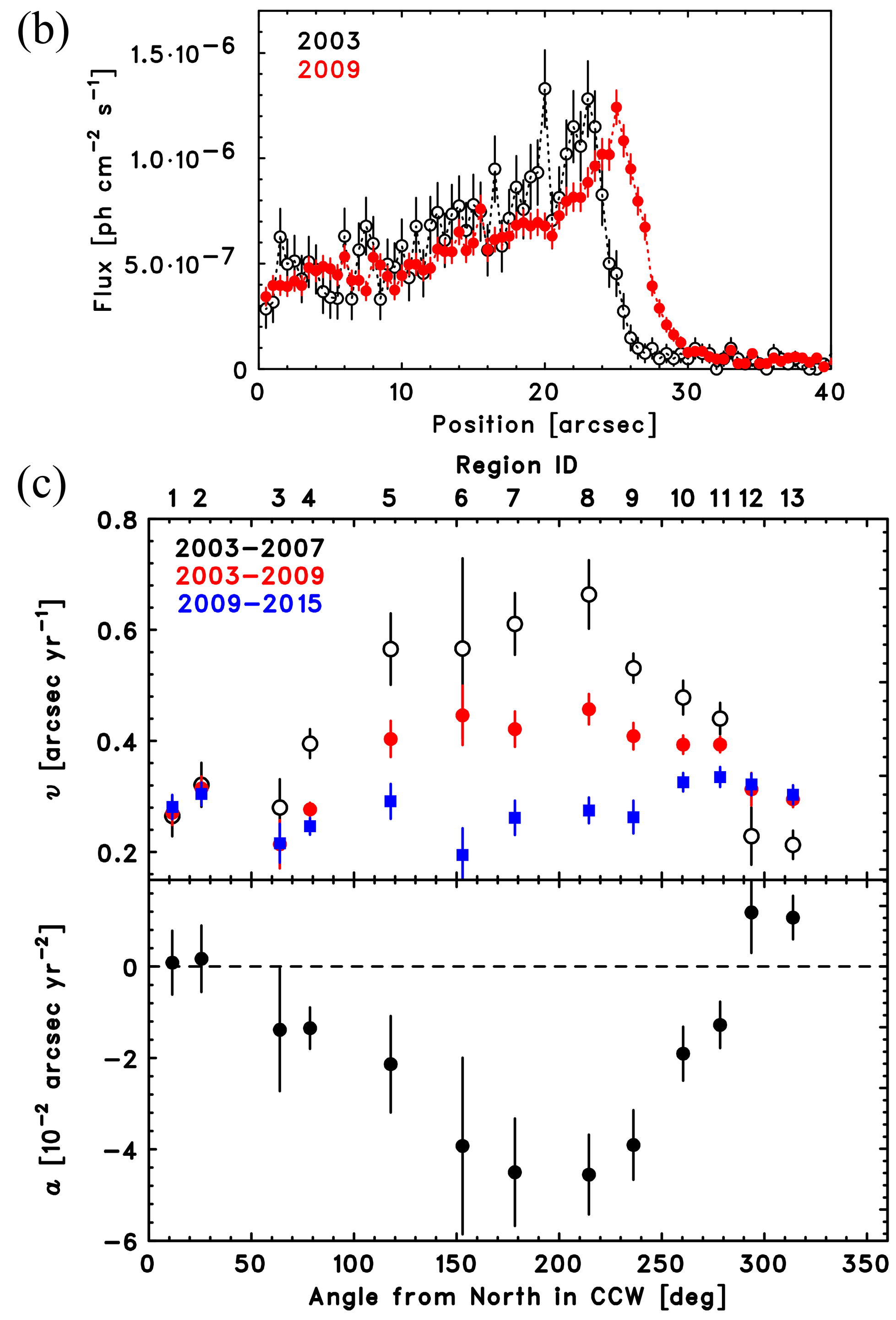

Figure 2. (a) Chandra ACIS flux image in the energy band between 4.1 keV and 6.1 keV. The red squares are regions used for expansion velocity measurements. (b) Projection along the shock front in Region 8. The black and red points indicate profiles obtained in 2003 and 2009, respectively. (c) Velocity (*top*) and acceleration (*bottom*) measured in each of the 13 regions. The acceleration is estimated assuming it is constant between 2003 and 2015. The horizontal axis represents angle from the north in counterclockwise. The distance to Tycho's SNR is assumed to be 2.5 kpc in converting arcsec to km.

3. Spectral Analysis with XMM-Newton

We performed spatially resolved X-ray spectroscopy with XMM-Newton. We extracted spectra from each square region in Figure 3a. An example of the spectra are presented in Figure 3b. To measure the line-of-sight velocities of the ejecta ($v_{\|}$), we fitted the spectra with a model consisting of two components with different velocities $v_r = v_{\|}$ and $v_b = -v_{\|}$, representing the red- and blue-shifted components of the ejecta of intermediate mass elements (IMEs: Si, S, S, Ar, and Ca) . From the obtained $v_{\|}$, we can estimate the expansion velocities of the ejecta $v_{\rm IME}$, by solving the inverse problem of Equation (1), which assumes that the SNR is spherically symmetric and the ejecta is filled between the reverse shock (RS) and the contact discontinuity (CD) with an expansion velocity of $v_{\rm IME}$. The estimated velocities $\bar{v}_{\rm IME}$ are plotted in Figure 4.

The obtained $\bar{v}_{\rm IME}$ keeps constant at ~ 4000 km s^{-1} within and $\sim 200''$ and then suddenly drops to ~ 1000 km s^{-1}. This is explained if the blast wave collided a dense gas wall, which is, in fact, demonstrated by our hydrodynamical simulation shown in Figure 6. The reflection shock generated by the collision is responsible for the low-velocity (~ 1000 km s^{-1}) component.

$$v_{\|}(x') = \begin{cases} \alpha(x')v_{\rm IME} + \beta(x')v_{\rm IME} & (0 \leqslant x' < r_{\rm RS}), \\ \gamma(x')v_{\rm IME} & (r_{\rm RS} \leqslant x' < r_{\rm ejecta}), \\ 0 & (r_{\rm ejecta} \leqslant x'), \end{cases} \quad (1)$$

$$\alpha(x') = \frac{r_{\rm RS}}{r_{\rm RS} + r_{\rm ejecta}} \sqrt{1 - \left(\frac{x'}{r_{\rm RS}}\right)^2} \quad (2)$$

$$\beta(x') = \frac{r_{\rm ejecta}}{r_{\rm RS} + r_{\rm ejecta}} \sqrt{1 - \left(\frac{x'}{r_{\rm ejecta}}\right)^2} \quad (3)$$

$$\gamma(x') = \sqrt{\frac{r_{\rm ejecta} - x'}{r_{\rm ejecta} + x'}}. \quad (4)$$

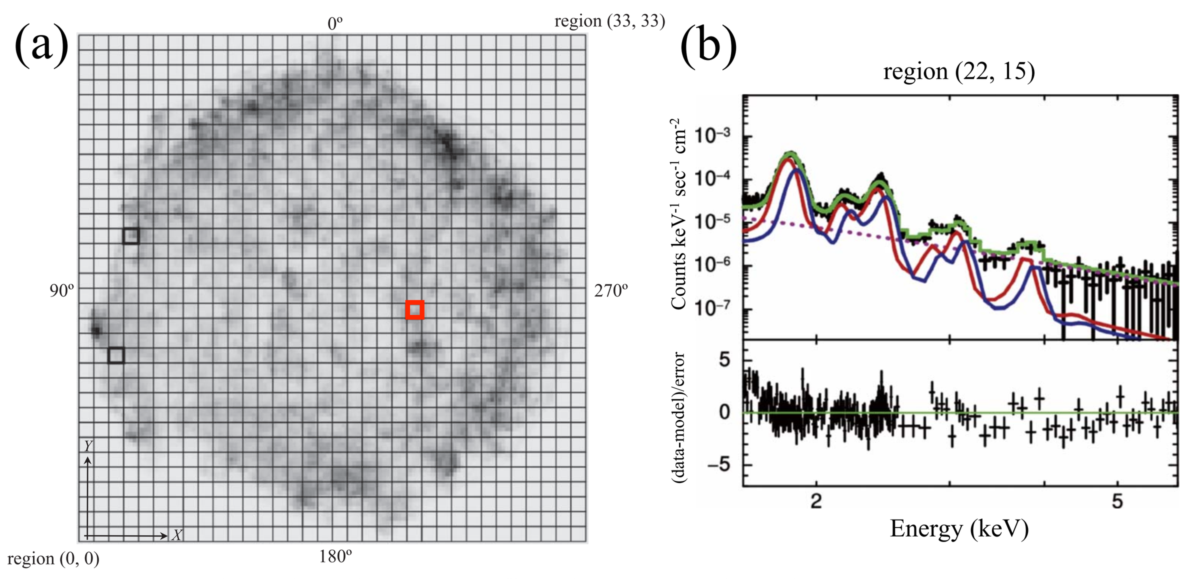

Figure 2. (a) Chandra ACIS flux image in the Si Kα band (1.80–1.92 keV) overlaid with the grids used for the spatially resolved spectroscopy. The definitions of the region number (X, Y) and the azimuthal angle θ (from the north counterclockwise) are also displayed. (b) Spectrum extracted from region (22, 15), which is indicated as a red square in the left figure. The red and blue curves represent red- and blue-shifted components, respectively. The green curve indicates their sum.

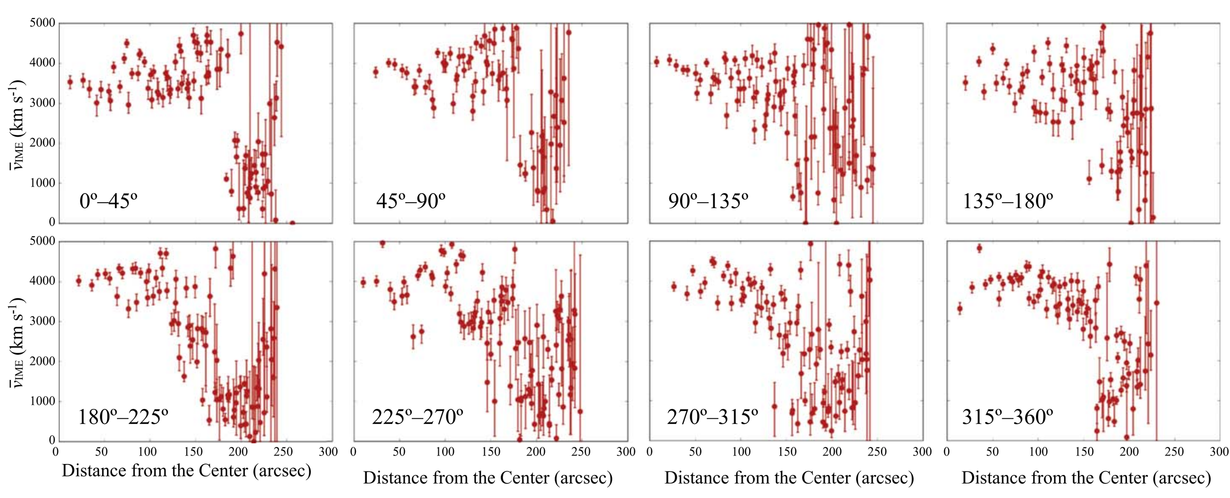

Figure 3. Radial profile of $\bar{v}_{\rm IME}$ for each octant of the remnant.

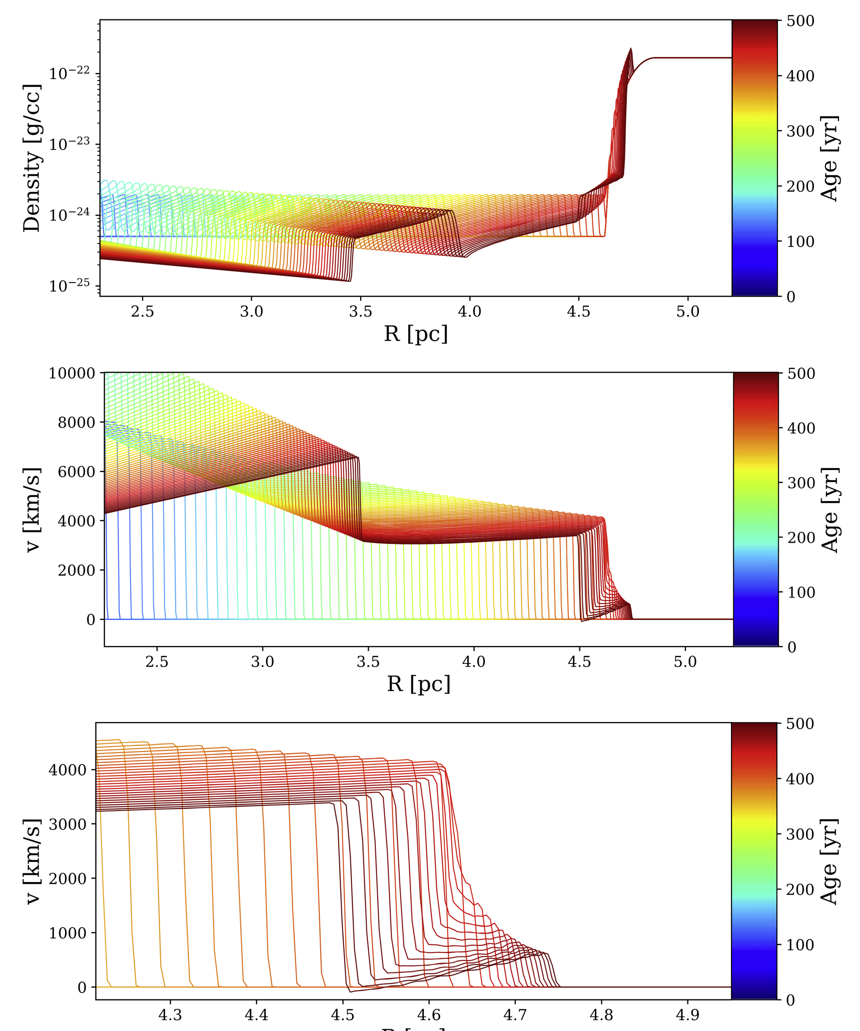

Figure 4. Results of our hydrodynamical simulation. The top and middle panels display the density and velocity profiles with radius, respectively. The bottom panel shows the zoom-in view of the velocity profile near the outer edge, where the reflection shock is generated.

4. Discussion

Both our imaging and spectral analyses implies that the blast wave of Tycho's SNR recently hit dense gas distributed in a wide range of azimuthal angle. A gas structure like cavity wall would be able to explain the result. Such a molecular gas structure is indeed found by Zhou et al. (2016), who analyzed data from IRAM 30 m telescope. (Figure 5).

A detection of such circumstellar materials has been regarded as a smoking gun for an SD progenitor of a SN Ia. The circumstellar materials strongly indicate that the progenitor should be a young system, making the DD scenario unlikely. In the SD scenario, a strong wind from the progenitor white dwarf during mass accretion (Hachisu et al. 1996) is one of the plausible mechanisms responsible for the formation of the cavity.

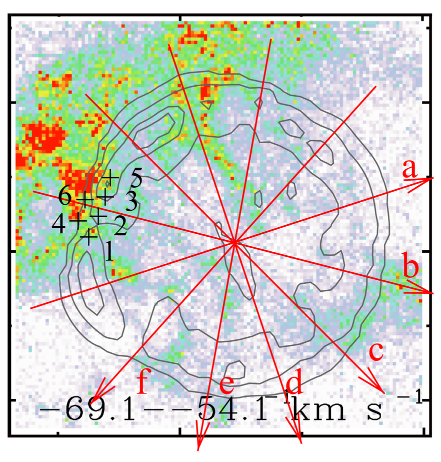

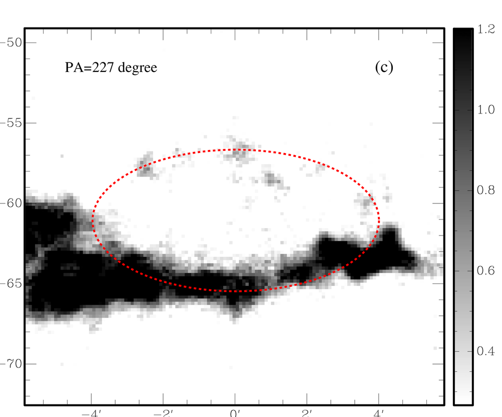

Figure 5. (Left) ^{12}CO (J = 2–1) intensity map in the velocity range −69.1 km s^{-1} to −54.1 km s^{-1} by Zhou et al. (2016). (Right) Position-velocity diagram along the red arrow "c" in the left panel. A bubble-like structure is clearly visible. Note that similar structures are found also along the other directions (adopted from Zhou et al. 2016).

See our papers for details of what is presented here.

Tanaka, T., Okuno, T., Uchida, H., Yamaguchi, H. Lee, S.-H., Maeda, K., Williams, B. J., 2021, ApJL, 906, L3 (Imaging Analysis with Chandra)

Uchida, H., Kasuga T. Maeda, K., Lee, S.-H., Tanaka, T., Bamba, A., 2024, ApJ, 962, 159 (Spectral Analysis with XMM-Newton)